



Stoner versus Heisenberg: Ultrafast exchange reduction and magnon generation during laser-induced demagnetization

Emrah Turgut,¹ Dmitriy Zusin,¹ Dominik Legut,^{2,3} Karel Carva,^{3,4} Ronny Knut,¹ Justin M. Shaw,⁵ Cong Chen,¹ Zhensheng Tao,¹ Hans T. Nembach,⁵ Thomas J. Silva,⁵ Stefan Mathias,⁶ Martin Aeschlimann,⁷ Peter M. Oppeneer,⁴ Henry C. Kapteyn,¹ Margaret M. Murnane,¹ and Patrik Grychtol¹

¹Department of Physics and JILA, University of Colorado, Boulder, Colorado 80309, USA

²IT4Innovations Center, VSB Technical University of Ostrava, CZ-70833 Ostrava, Czech Republic

³Department of Condensed Matter Physics, Charles University, CZ-12116 Prague 2, Czech Republic

⁴Department of Physics and Astronomy, Uppsala University, P.O. Box 516, S-75120 Uppsala, Sweden

⁵Electromagnetics Division, National Institute of Standards and Technology, Boulder, Colorado 80305, USA

⁶I. Physikalisches Institut, Georg-August-Universität Göttingen, D-37077 Göttingen, Germany

⁷University of Kaiserslautern and Research Center OPTIMAS, D-67663 Kaiserslautern, Germany

(Received 6 May 2016; revised manuscript received 18 November 2016; published 28 December 2016)

Understanding how the electronic band structure of a ferromagnetic material is modified during laser-induced demagnetization on femtosecond time scales has been a long-standing question in condensed matter physics. Here, we use ultrafast high harmonics to measure time-, energy-, and angle-resolved M -edge magnetic asymmetry spectra for Co films after optical pumping to induce ultrafast demagnetization. This provides a complete data set that we can compare with advanced *ab initio* magneto-optical calculations. Our analysis identifies that the dominant mechanisms contributing to ultrafast demagnetization on time scales up to several picoseconds are a transient reduction in the exchange splitting and the excitation of ultrafast magnons. Surprisingly, we find that the magnon contribution to ultrafast demagnetization is already strong on subpicosecond time scales, while the reduction in exchange splitting persists to several picoseconds.

DOI: [10.1103/PhysRevB.94.220408](https://doi.org/10.1103/PhysRevB.94.220408)

Understanding the interaction of light with magnetic materials has been a subject of intense investigations, because it is interesting both for an understanding of fundamental excitations, as well as for advancing data storage technologies [1]. When excited by intense femtosecond laser pulses, many ferromagnetic materials demagnetize on subpicosecond time scales [2]. However, a consensus as to the dominant physical mechanisms responsible for ultrafast demagnetization remains elusive, despite extensive theoretical and experimental studies of the elementary nonequilibrium interactions between photons, spins, charges, and phonons [3–6]. One reason for this lack of consensus is the absence of unambiguous experimental data and probes that would make it possible to discriminate between the various microscopic mechanisms contributing to far-from-equilibrium dynamics in magnetic materials [7–10]. Fortunately, new techniques with improved capabilities are now available to address this challenge. Advances in extreme ultraviolet (EUV) high harmonic generation (HHG) light sources, for example, make it possible to probe ultrafast electron and spin dynamics of multiple elements in alloys and multilayers simultaneously over their entire absorption edges, thereby capturing microscopic processes with an unprecedented level of detail [11–20]. Several past experiments successfully used HHG to uncover how strong exchange interactions influence dynamics in magnetic alloys, and identified the importance of both ultrafast superdiffusive spin currents and spin scattering in magnetic multilayers [13–16].

One mechanism proposed for ultrafast demagnetization is a reduction in the magnitude of the local atomic moment by *longitudinal spin-flip processes* resulting from spin-orbit interactions present in Elliott-Yafet electron-phonon scattering [21], or from Stoner excitations [22]. This picture is

rooted in the Stoner model of itinerant ferromagnetism, which assumes that the atomic magnetic moment is proportional to the exchange splitting ε_{ex} of the majority and minority bands [23,24]. However, the Stoner model does not provide a complete picture of ferromagnetism, insofar as it does not naturally include correlated spin excitations that are the eigenstates of the Heisenberg Hamiltonian, namely, magnons. Such quantized, delocalized, *transverse excitations* also reduce the net magnetization, albeit with correlation lengths that can be many orders of magnitude longer than what are expected for longitudinal excitations [25,26].

Transverse spin fluctuations have been proposed as an alternative explanation of ultrafast laser-induced demagnetization [8,9,27–31]. For example, Carpene *et al.* interpreted an apparent time delay between reductions in the time-resolved reflectivity and the magneto-optic Kerr effect (MOKE) as evidence of magnon generation on 100 fs time scales [28]. It was also suggested that spin-resolved two-photon photoemission measurements might provide indirect evidence for magnon generation facilitated by hot electron decay [9]. Indeed, it has been well established by both inelastic neutron scattering and spin-polarized electron energy loss spectroscopy that magnon lifetimes can be extremely short, in the femtosecond range for Co, when the magnon dispersion overlaps with the continuum of Stoner excitations [32,33]. Hence, one could expect that transverse excitations also contribute to ultrafast demagnetization.

In this Rapid Communication, to investigate the dominant mechanisms contributing to ultrafast demagnetization, we measure the time-, energy-, and angle-resolved EUV transverse-MOKE (T-MOKE) response across the entire $M_{2,3}$ absorption edges of a Co film (hcp) after excitation with a femtosecond laser pulse. Since EUV MOKE probes the entire

demagnetization response of the $3d$ bands, this provides a complete data set which we can compare with first-principles magneto-optical calculations. We find that both longitudinal and transverse processes contribute to demagnetization in Co on time scales up to several picoseconds. Surprisingly, the magnon contribution to demagnetization is dominant on very short (700 fs) time scales, while the reduction in exchange splitting persists to several picosecond time scales. Finally, this work demonstrates that each of these mechanisms has a particular magneto-optical “fingerprint” making identification possible, as suggested 40 years ago by Erskine and Stern. They proposed that measuring the EUV magneto-optic response across the entire $M_{2,3}$ absorption edges contains all the spin-dependent information about the electronic structure in the conduction band [34]. We demonstrate that this is possible even for dynamically out-of-equilibrium materials.

In our experiment, 40 fs near-infrared laser pulses are used to excite a thin film Co grating sample [see Fig. 1(a)]. The resultant dynamics are then probed using broadband HHG EUV pulses (<10 fs) that are jitter-free synchronized with the laser pump pulses. The bandwidth of the temporally and spatially coherent EUV probe beam spans from 40 to 72 eV, accessing the entire $M_{2,3}$ absorption edges of the $3d$ ferromagnets. The sample (Si substrate/150 nm SiO_2 /3 nm Ta/10 nm Co/3 nm Si_3N_4) was lithographically patterned to form a grating (500 lines/mm) spectrally dispersing the EUV HHG beam, which is then detected by an x-ray camera. Note that because our thin Co sample was grown on an insulating material, it precludes thermal transport as well as the generation of superdiffusive spin currents that also can contribute to ultrafast demagnetization [35]. The incident angle (θ) of the probe beam was varied between 37.5° and 52.5° to record the angle- and energy-resolved magnetic asymmetry A , which is approximately linearly proportional to the magnetization [36,37].

We first characterized the average and normalized dynamic magnetic response Δm_{avg} of Co by recording A in fine time steps at $\theta = 45^\circ$ and integrating A in a defined energy interval (57–61 eV). The result [Fig. 1(b)] shows demagnetization and partial recovery [2]. As indicated by red arrows, two points in time were selected for the subsequent angle- and energy-resolved asymmetry measurements: first, at the maximum of demagnetization around 0.7 ps, when the electronic system has thermalized to a hot Fermi-Dirac distribution [38–40], and second, around 3 ps, when the magnetization has recovered by 50% and electron-phonon relaxation has begun.

To investigate the origin of the reduction in the magneto-optical signal, we performed *ab initio* calculations of the EUV magneto-optical response at the hcp Co $M_{2,3}$ absorption edges. Our relativistic calculations are based on the linear-response theory for the dielectric tensor ϵ_{ij} including the effects of semi-core-level exchange splitting and hybridization and spin-orbit interaction [41]. In our calculations, the influence of the electronic structure on A was simulated by modifying the electron temperature, and reducing the exchange splitting assuming a laser-induced redistribution of electrons across the energy bands (see Fig. 2). Moreover, we investigated the effect of magnons by computing the magneto-optical response for noncollinear magnetic configurations. Their influence was found to be very similar to simply multiplying the off-diagonal

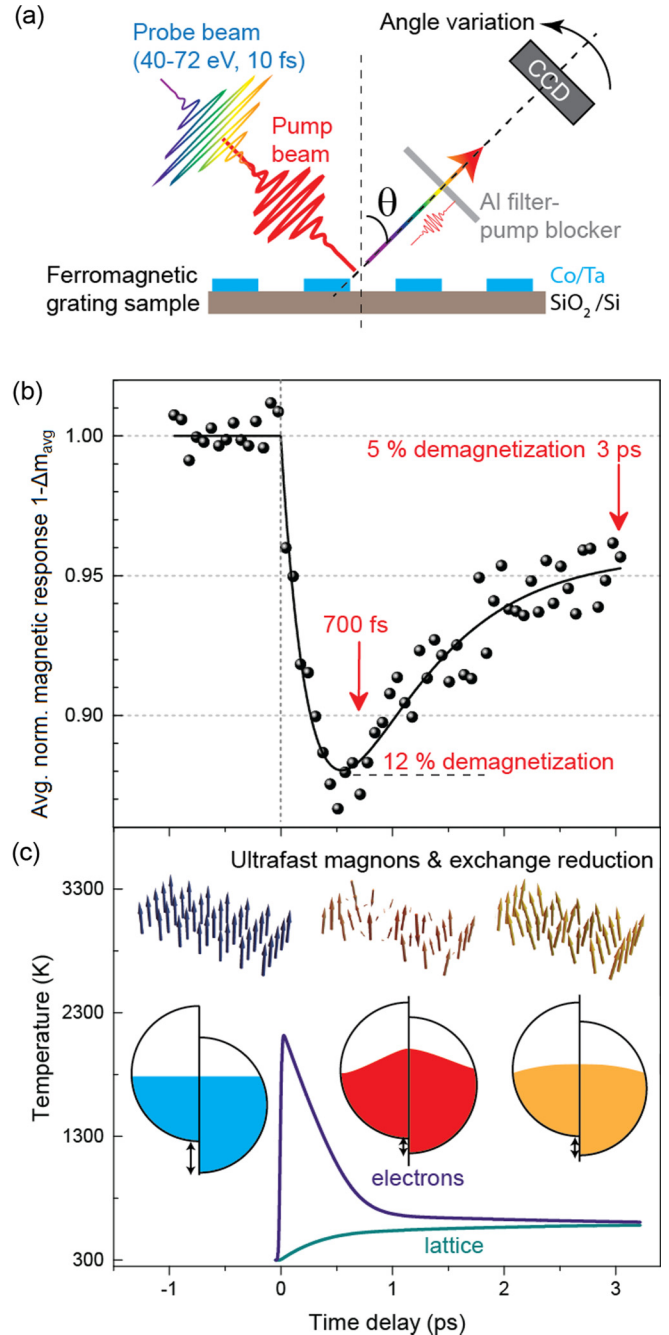


FIG. 1. (a) Setup for time-, energy-, and angle-resolved T-MOKE. (b) Transient average normalized magneto-optic response. (c) Evolution of the electron and lattice temperatures estimated from the three-temperature model (lines). The inset illustrates the microscopic mechanisms behind laser-induced demagnetization dynamics: Ultrafast magnons (top), and exchange reduction and thermal smearing (middle panels).

dielectric tensor element ϵ_{xy} by a constant factor before computing A [see Ref. [34] and the Supplemental Material (SM) [42]]. Note that in all simulations, the $3p$ core states are not treated as rigid, since the feedback effect of the modified valence states upon the core levels is self-consistently included. Although we do not calculate the full time evolution, we capture instantaneous snapshots of the demagnetization theoretically to simulate the measured time-, energy-,

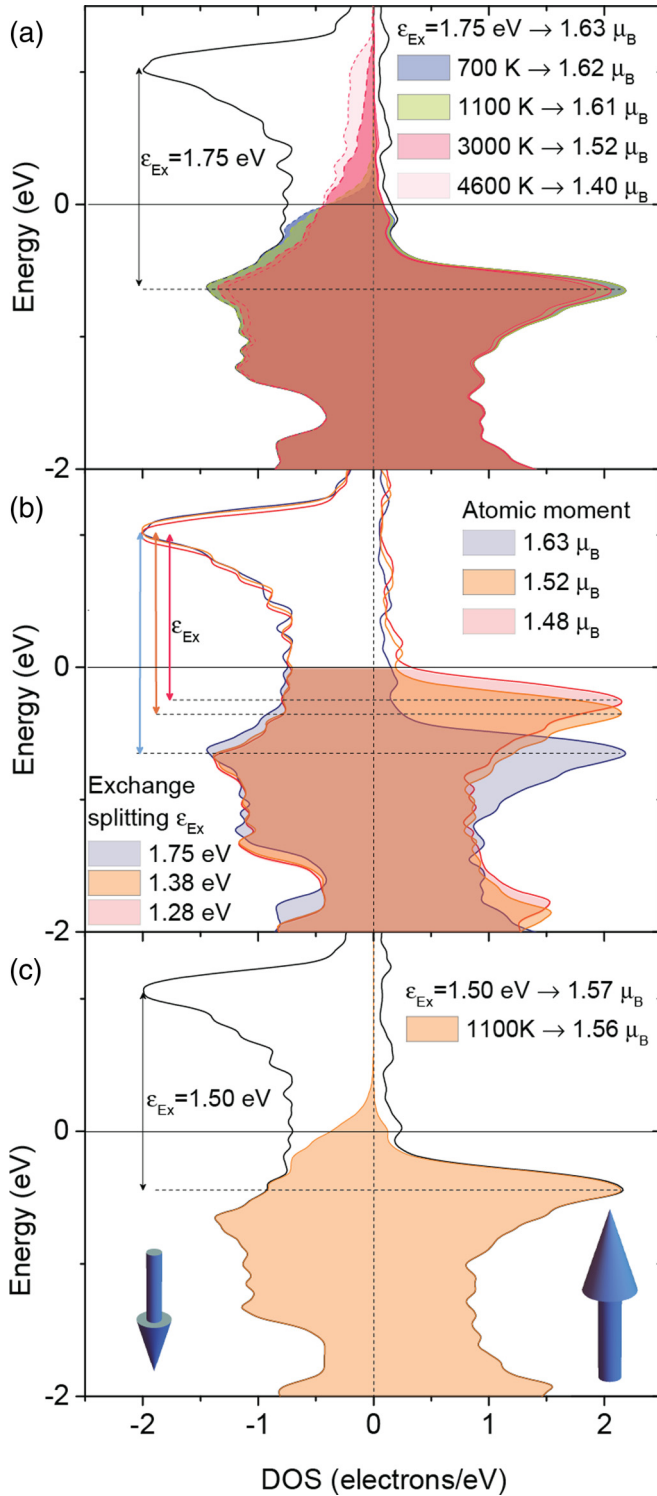


FIG. 2. (a) *Ab initio* calculations of the spin-dependent density of states in Co at elevated electron temperatures (700, 1100, 3000, and 4600 K), (b) with reduced exchange splitting ϵ_{Ex} , and (c) reduced exchange splitting in combination with an elevated electron temperature of 1100 K.

and angle-resolved magnetic asymmetry spectra for the Co film. For each electron temperature and exchange splitting (cf. Fig. 2), the off-diagonal elements of the dielectric tensor ϵ_{xy} are derived. They are then used to compute A using a multi-

layer code [43]. We compared theory with experiment using a least-square-fit algorithm, where the contribution of transverse excitations is a free fitting parameter. The root-mean-square (rms) deviation serves as a quantitative measure of the fit. The measured and calculated asymmetry spectra, before laser excitation, are in good agreement with one another, as seen in Fig. 3.

The (normalized) atomic moment is reduced by Δm_e due to the thermal smearing, Δm_l due to longitudinal spin excitations, and Δm_t due to transverse spin excitations, i.e., magnon generation. Thus, the change in the total normalized moment will be given by $\Delta m = \Delta m_e + \Delta m_l + \Delta m_t$, where $\Delta m_x = \mu_x/\mu$, and where μ is the moment before time zero at 300 K, with $x = e, l, t$. As can be seen from Fig. 1(b), the averaged magneto-optical response of the Co film drops by a fractional $\Delta m_{\text{avg}} = 0.12$ and 0.05 at 0.7 and 3 ps, respectively, after excitation with an absorbed pump fluence of 1.3 mJ/cm^2 . For this laser fluence, the maximum initial electron temperature is $T_e = 2300 \text{ K}$, decreasing to approximately 1000 K by 700 fs [see Fig. 1(c) and SM for results of the phenomenological three-temperature model].

Based on these estimates, we first exclude the possibility of demagnetization arising only from an elevated electron temperature. At $T_e = 1100 \text{ K}$, $\Delta m_e = 0.0008$, which is an order of magnitude less than what we measure. Indeed, a temperature exceeding 4000 K would be needed to achieve $\Delta m_e = 0.12$ at 0.7 ps, which is unphysically high for our laser fluence (see SM). Next, we calculate the dynamic differential changes in angle-resolved asymmetry, $A(t) - A(t < 0)$, at $t = 0.7 \text{ ps}$ and at $t = 3 \text{ ps}$, by varying T_e , ϵ_{Ex} , and the magnon excitations with respect to the unperturbed ground state. We then compared the calculated spectra with the experimental data in Figs. 3(b) and 3(c) by employing a least-square-fit algorithm. The best fits are shown in Figs. 3(e) and 3(f), while a summary of the rms analysis is graphically displayed in Figs. 3(h) and 3(i) (see SM). Using the same fitting procedure, we extract unphysically high T_e if we assume that demagnetization is induced only by magnons or only by exchange reduction. Moreover, either mechanism alone cannot reproduce the observed magnitude of demagnetization (see SM).

To achieve good agreement between experiment and theory, we must include both longitudinal and transverse spin excitations, along with a much smaller atomic moment reduction due to thermal smearing. On short time scales (0.7 ps, $\Delta m_{\text{avg}} = 0.12 \pm 0.01$) the exchange splitting is reduced by $\Delta \epsilon_{\text{Ex}} = 0.26 \text{ eV}$ for an electron temperature around 1120 K, such that $\Delta m_l = 0.032 \pm 0.013$, which accounts for approximately $\frac{1}{4}$ of the measured $\Delta m_{\text{avg}} = 0.12$. This is accompanied by an electronic contribution of $\Delta m_e = 0.008$ and a magnon-generation contribution of $\Delta m_t = 0.073 \pm 0.006$, or $\frac{2}{3}$ of the observed magnetization reduction, which results in a total reduction of the magnetic moment to about $1.44 \mu_B/\text{atom}$ ($\Delta m = 0.115 \pm 0.014$). On longer time scales (3 ps, $\Delta m_{\text{avg}} = 0.05 \pm 0.01$), the lower electron temperature allows a partial recovery of the exchange reduction to about $\Delta \epsilon_{\text{Ex}} = 0.15 \text{ eV}$ ($\Delta m_l = 0.021 \pm 0.011$), which is accompanied by a magnon contribution of $\Delta m_t = 0.028 \pm 0.004$ resulting in a total reduction of the magnetic moment to about $1.54 \mu_B/\text{atom}$, or $\Delta m = 0.049 \pm 0.012$. We conclude that the changes in

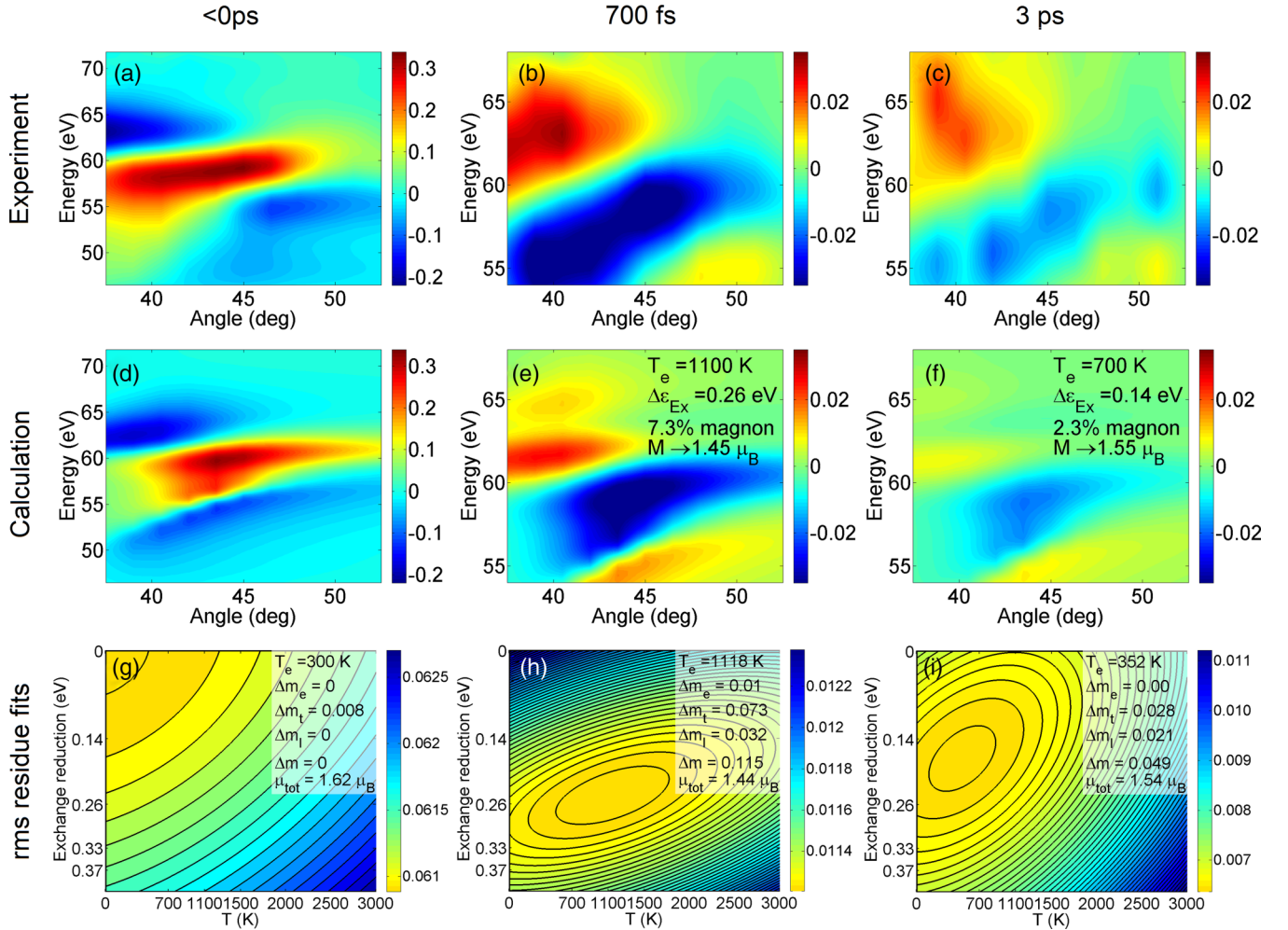


FIG. 3. Comparison of the (a) experimental and (d) theoretical angle- and energy-resolved T-MOKE asymmetries before laser excitation. Comparison of the (b), (c) experimental and (e), (f) theoretical differential asymmetry spectra at 0.7 and 3 ps. The measured differential spectra (b) and (c) at both delay times exhibit distinct qualitative differences from the spectrum at time zero (a). (e) and (f) show specific examples of calculated spectra near the optimal values determined from the least-squares fit. Last row (g)–(i): Contour plots of quadratic fits to rms residues resulting from independent fitting of *ab initio* calculated spectra to measured spectra. It can be clearly seen how the Co film is excited by a femtosecond laser pulse from (g) <0 ps to (h) 0.7 ps and how it relaxes back towards equilibrium from (h) 0.7 ps to (i) 3 ps. In (g), $\Delta m_l = 0.008$ is based on Ref. [44].

the magneto-optical signal at 3 ps originate from roughly equal contributions of exchange splitting and nonequilibrium magnon excitation. This finding is interesting, since one might expect that thermalization would mainly support magnon generation rather than longitudinal excitations. However, our calculations confirm that the total energy costs associated with a local moment reduction ($\Delta E = 1.4$ meV for $\Delta m_l = 0.021$ and $\Delta E = 2.6$ meV for $\Delta m_l = 0.032$) are comparable to those of magnons. Thus, the Co local moment is apparently very susceptible to perturbations and a significant contribution to the demagnetization from its decrease is therefore possible. We also note that the exchange and magnon contributions are not strongly dependent on the electron temperature (see SM).

Our observation of fast magnon generation that accounts for $\sim \frac{2}{3}$ of the magnetization reduction at 700 fs is surprising. It is important to note, however, that our sample consists of a Co film on an insulating substrate. This means that any laser-generated superdiffusive spin currents cannot escape the

film, and hence other spin dissipation channels such as ultrafast magnon generation can come into play. Moreover, while a persistent reduction of the exchange splitting for times >3 ps might not be expected, strong coupling between nonthermal, high energy transverse (magnons) and longitudinal (Stoner) excitations in the 100 meV range might lead to a comparable thermalization time for both excitations.

The possible contributions of reduced exchange splitting and magnon excitation have been discussed over the last years, but without strong consensus to date [9,10,22,28,30,39,45–48]. Some authors observe a change of exchange splitting during ultrafast demagnetization [39,46–48], while others do not [30]. One source of confusion has been that it had not been realized that the behavior of magnetic films on metallic substrates is different, since spin currents can modify the occupations of the spin-polarized bands. Also, different probes measure different parts of bands in the Brillouin zone and are thus sensitive to different contributions [10]. In addition,

the behavior of $4f$ ferromagnets is more involved than in pure $3d$ systems due to coupled reactions of $5d$ and $4f$ spin-polarized electrons [46–48]. Recently, Carpené *et al.* used femtosecond magneto-optical and reflectivity spectroscopy to study the demagnetization of an Fe film, and concluded that the process is dominated by transversal spin excitations and not changes in exchange splitting [30]. Our results for Co uncover the importance of both magnon excitation and exchange reduction. The fact that Fe has a larger exchange splitting than Co might play a role here, making transverse spin excitations energetically more favorable in Fe. Also, in contrast to the small spectral region probed by Carpené *et al.*, broadband HHG makes it possible to probe the entire Co $M_{2,3}$ edges, significantly increasing its sensitivity to changes in the band structure.

In summary, we present a fresh perspective on the long-standing question of which microscopic mechanisms are responsible for ultrafast laser-driven demagnetization of ferromagnets. By combining ultrafast time-, energy-, and angle-resolved measurements of the transverse MOKE at the Co $M_{2,3}$ -absorption edges with advanced *ab initio* magneto-optical calculations, we conclude that two mechanisms are dominant for our sample structure and geometry with roughly equal contributions: a transient reduction in the exchange

splitting, and ultrafast magnon generation. Surprisingly, we find that the magnon contribution to ultrafast demagnetization is already strong on subpicosecond time scales, while the reduction in exchange splitting persists to several picosecond time scales. Finally, our findings demonstrate the original conjecture by Erskine and Stern, that each of these mechanisms has a particular magneto-optical “fingerprint” that makes identification possible [34].

This work was done at JILA. M.M.M. and H.C.K. acknowledge support from the Department of Energy (DOE) Office of Basic Energy Sciences X-Ray Scattering Program Award No. DE-SC0002002 and a Gordon and Betty Moore Foundation EPiQS Award through Grant No. GBMF4538. R.K. and P.M.O. acknowledge the Swedish Research Council (VR) for financial support. K.C. and P.M.O. acknowledge support from the EU Seventh Framework Program (Grant No. 281043, FemtoSpin) and the Wallenberg Foundation (Grant No. 2015.0060). M.A. acknowledges support from the German Science Foundation through the SFB/TRR 173 “Spin+X” (Project A02). K.C. acknowledges the Czech Science Foundation (Grant No. 15-08740Y). D.L. acknowledges support from IT4Innovations Project No. LM2015070 and COST Action MP1306 EUSpec.

-
- [1] S. Mangin, M. Gottwald, C.-H. Lambert, D. Steil, V. Uhlíř, L. Pang, M. Hehn, S. Alebrand, M. Cinchetti, G. Malinowski, Y. Fainman, M. Aeschlimann, and E. Fullerton, *Nat. Mater.* **13**, 286 (2014).
- [2] E. Beaurepaire, J.-C. Merle, A. Daunois, and J.-Y. Bigot, *Phys. Rev. Lett.* **76**, 4250 (1996).
- [3] G. P. Zhang, W. Hübner, G. Lefkidis, Y. Bai, and T. F. George, *Nat. Phys.* **5**, 499 (2009).
- [4] J.-Y. Bigot, M. Vomir, and E. Beaurepaire, *Nat. Phys.* **5**, 515 (2009).
- [5] U. Bovensiepen, *Nat. Phys.* **5**, 461 (2009).
- [6] A. Kirilyuk, A. Kimel, and T. Rasing, *Rev. Mod. Phys.* **82**, 2731 (2010).
- [7] A. Scholl, L. Baumgarten, R. Jacquemin, and W. Eberhardt, *Phys. Rev. Lett.* **79**, 5146 (1997).
- [8] M. Cinchetti, M. Sánchez Albaneda, D. Hoffmann, T. Roth, J.-P. Wüstenberg, M. Krauß, O. Andreyev, H. C. Schneider, M. Bauer, and M. Aeschlimann, *Phys. Rev. Lett.* **97**, 177201 (2006).
- [9] A. B. Schmidt, M. Pickel, M. Donath, P. Buczek, A. Ernst, V. P. Zhukov, P. M. Echenique, L. M. Sandratskii, E. V. Chulkov, and M. Weinelt, *Phys. Rev. Lett.* **105**, 197401 (2010).
- [10] A. Weber, F. Pressacco, S. Günther, E. Mancini, P. M. Oppeneer, and C. H. Back, *Phys. Rev. B* **84**, 132412 (2011).
- [11] C. La-O-Vorakiat, M. Siemens, M. M. Murnane, H. Kapteyn, S. Mathias, M. Aeschlimann, P. Grychtol, R. Adam, C. M. Schneider, J. M. Shaw, H. Nembach, and T. J. Silva, *Phys. Rev. Lett.* **103**, 257402 (2009).
- [12] C. La-O-Vorakiat, E. Turgut, C. Teale, H. Kapteyn, M. Murnane, S. Mathias, M. Aeschlimann, C. M. Schneider, J. Shaw, H. Nembach, and T. Silva, *Phys. Rev. X* **2**, 011005 (2012).
- [13] S. Mathias, C. La-O-Vorakiat, P. Grychtol, P. Granitzka, E. Turgut, J. Shaw, R. Adam, H. Nembach, M. Siemens, S. Eich, C. M. Schneider, T. J. Silva, M. Aeschlimann, M. Murnane, and H. Kapteyn, *Proc. Natl. Acad. Sci. USA* **109**, 4792 (2012).
- [14] D. Rudolf, C. La-O-Vorakiat, M. Battiato, R. Adam, J. M. Shaw, E. Turgut, P. Maldonado, S. Mathias, P. Grychtol, H. T. Nembach, T. J. Silva, M. Aeschlimann, H. C. Kapteyn, M. M. Murnane, C. M. Schneider, and P. M. Oppeneer, *Nat. Commun.* **3**, 1037 (2012).
- [15] E. Turgut, C. La-O-Vorakiat, J. Shaw, P. Grychtol, H. Nembach, D. Rudolf, R. Adam, M. Aeschlimann, C. M. Schneider, T. J. Silva, M. M. Murnane, H. C. Kapteyn, and S. Mathias, *Phys. Rev. Lett.* **110**, 197201 (2013).
- [16] S. Mathias, C. La-O-Vorakiat, J. Shaw, E. Turgut, P. Grychtol, R. Adam, D. Rudolf, H. Nembach, T. Silva, M. Aeschlimann, C. Schneider, H. Kapteyn, and M. Murnane, *J. Electron Spectrosc. Relat. Phenom.* **189**, 164 (2013).
- [17] N. Bergéard, V. López-Flores, V. Halté, M. Hehn, C. Stamm, N. Pontius, E. Beaurepaire, and C. Boeglin, *Nat. Commun.* **5**, 3466 (2014).
- [18] O. Kfir, P. Grychtol, E. Turgut, R. Knut, D. Zusin, D. Popmintchev, T. Popmintchev, H. Nembach, J. Shaw, A. Fleischer, H. C. Kapteyn, M. M. Murnane, and O. Cohen, *Nat. Photon.* **9**, 99 (2015).
- [19] D. Hickstein, F. Dollar, P. Grychtol, J. Ellis, R. Knut, C. Hernández-García, D. Zusin, C. Gentry, J. Shaw, T. Fan, K. Dorney, A. Becker, A. Jaroń-Becker, H. C. Kapteyn, M. M. Murnane, and C. Durfee, *Nat. Photon.* **9**, 743 (2015).
- [20] T. Fan, P. Grychtol, R. Knut, C. Hernández-García, D. Hickstein, D. Zusin, C. Gentry, F. Dollar, C. Mancuso, C. Hogle, O. Kfir, D. Legut, K. Carva, J. Ellis, K. Dorney, C. Chen, O. Shpyrko, E. Fullerton, O. Cohen, P. M. Oppeneer, D. B. Milosevic, A. Becker, A. A. Jaron-Becker, T. Popmintchev, M. M. Murnane, and H. C. Kapteyn, *Proc. Natl. Acad. Sci. USA* **112**, 14206 (2015).

- [21] B. Koopmans, G. Malinowski, F. Dalla Longa, D. Steiauf, M. Fähnle, T. Roth, M. Cinchetti, and M. Aeschlimann, *Nat. Mater.* **9**, 259 (2010).
- [22] B. Y. Mueller, A. Baral, S. Vollmar, M. Cinchetti, M. Aeschlimann, H. C. Schneider, and B. Rethfeld, *Phys. Rev. Lett.* **111**, 167204 (2013).
- [23] E. C. Stoner, *Proc. R. Soc. London, Ser. A* **165**, 372 (1938).
- [24] H. Ibach, *Physics of Surfaces and Interfaces* (Springer, Berlin, 2006).
- [25] C. Herring and C. Kittel, *Phys. Rev.* **81**, 869 (1951).
- [26] M. P. Gokhale and D. L. Mills, *Phys. Rev. B* **49**, 3880 (1994).
- [27] U. Atxitia, O. Chubykalo-Fesenko, N. Kazantseva, D. Hinzke, U. Nowak, and R. W. Chantrell, *Appl. Phys. Lett.* **91**, 232507 (2007).
- [28] E. Carpene, E. Mancini, C. Dallera, M. Brenna, E. Puppini, and S. De Silvestri, *Phys. Rev. B* **78**, 174422 (2008).
- [29] N. Kazantseva, U. Nowak, R. W. Chantrell, J. Hohlfeld, and A. Rebei, *Europhys. Lett.* **81**, 27004 (2008).
- [30] E. Carpene, H. Hedayat, F. Boschini, and C. Dallera, *Phys. Rev. B* **91**, 174414 (2015).
- [31] D. Hinzke, U. Atxitia, K. Carva, P. Nieves, O. Chubykalo-Fesenko, P. M. Oppeneer, and U. Nowak, *Phys. Rev. B* **92**, 054412 (2015).
- [32] H. A. Mook and D. Paul, *Phys. Rev. Lett.* **54**, 227 (1985).
- [33] R. Vollmer, M. Etzkorn, P. Kumar, H. Ibach, and J. Kirschner, *Phys. Rev. Lett.* **91**, 147201 (2003).
- [34] J. Erskine and E. Stern, *Phys. Rev. B* **12**, 5016 (1975).
- [35] M. Battiato, K. Carva, and P. M. Oppeneer, *Phys. Rev. Lett.* **105**, 027203 (2010).
- [36] P. M. Oppeneer, in *Magneto-Optical Kerr Spectra*, edited by K. H. J. Buschow, Handbook of Magnetic Materials Vol. 13 (Elsevier, Amsterdam, 2001), pp. 229–422.
- [37] P. Grychtol, R. Adam, S. Valencia, S. Cramm, D. Bürgler, and C. M. Schneider, *Phys. Rev. B* **82**, 054433 (2010).
- [38] C. Guo, G. Rodriguez, and A. J. Taylor, *Phys. Rev. Lett.* **86**, 1638 (2001).
- [39] H. S. Rhie, H. Dürr, and W. Eberhardt, *Phys. Rev. Lett.* **90**, 247201 (2003).
- [40] M. Lisowski, P. Loukakos, U. Bovensiepen, J. Stähler, C. Gahl, and M. Wolf, *Appl. Phys. A* **78**, 165 (2004).
- [41] S. Valencia, A. Kleibert, A. Gaupp, J. Ruzs, D. Legut, J. Bansmann, W. Gudat, and P. M. Oppeneer, *Phys. Rev. Lett.* **104**, 187401 (2010).
- [42] See Supplemental Material at <http://link.aps.org/supplemental/10.1103/PhysRevB.94.220408> for more details on our experimental and numerical methods, analysis and results.
- [43] V. W. Biricik, *Appl. Opt.* **28**, 1501 (1989).
- [44] S. V. Halilov, H. Eschrig, A. Y. Perlov, and P. M. Oppeneer, *Phys. Rev. B* **58**, 293 (1998).
- [45] A. Fognini, T. U. Michlmayr, G. Salvatella, C. Wetli, U. Ramsperger, T. Bähler, F. Sorgenfrei, M. Beye, A. Eschenlohr, N. Pontius, C. Stamm, F. Hieke, M. Dell’Angela, S. de Jong, R. Kukreja, N. Gerasimova, V. Rybnikov, A. Al-Shemmary, H. Redlin, J. Raabe, A. Föhlisch, H. A. Dürr, W. Wurth, D. Pescia, A. Vaterlaus, and Y. Acremann, *Appl. Phys. Lett.* **104**, 032402 (2014).
- [46] M. Teichmann, B. Frietsch, K. Dobrich, R. Carley, and M. Weinelt, *Phys. Rev. B* **91**, 014425 (2015).
- [47] B. Andres, M. Christ, C. Gahl, M. Wietstruk, M. Weinelt, and J. Kirschner, *Phys. Rev. Lett.* **115**, 207404 (2015).
- [48] B. Frietsch, J. Bowlan, R. Carley, M. Teichmann, S. Wienholdt, D. Hinzke, U. Nowak, K. Carva, P. M. Oppeneer, and M. Weinelt, *Nat. Commun.* **6**, 8262 (2015).